



True Amplitude Depth Migration with Curvelets

Hamideh Sanavi, and Peyman P. Moghaddam

Earthquake Research Center, Ferdowsi University of Mashhad, Iran

Summary

In this paper, we propose a true amplitude solution to the seismic imaging problem. We derive a diagonal scaling approach in curvelet domain for the normal operator approximation, which is based on the fact that curvelets remain approximately invariant under the action of operator. We use curvelets as essential tools for both approximation and inversion.

Our method produces a good resolution of the conflicting dips reflectors, reproduces true reflector amplitudes and compensates for incomplete illumination in seismic images. Our method is tested with a reverse-time 'wave equation' migration code simulating the acoustic wave equation on BP 2004 synthetic dataset.

Introduction

Despite the fact that modern depth migrations can accurately position reflecting surfaces in the Earth subsurface, they often do not correctly resolve the amplitudes. This is true, even when the accurate knowledge of the velocity model is available. Many approaches have been proposed for true-amplitude migration problem, which generally fall in three main categories.

First is "in the migration" correction approach of correcting amplitudes, where corrections are made during migration by applying imaging conditions that take into account reflector amplitudes (see e.g. Yang et.al. 2015; Da Silva et.al. 2011; Costa and Novais 2009; Chattopadhyay & McMechan, 2008).

Second, the fact that the migration operator is the adjoint but not the (pseudo)inverse of the scattering operator, which theoretically generates the data, (see e.g. Guitton, 2004; Claerbout, 1985; Gray, 1997; Symes, 2007), leads to a variety of algorithms for true amplitude migration which iteratively (using Lanczos or other linear algebra methods) update the migrated image to minimize the error between observed and modeled data (see e.g. Trad, 2017; Lu et. al 2017, Kuel and Sacchi, 2003).

Third, there are so called image-to-image scaling methods, where the Hessian (normal operator) is approximated through a scaling method. The scaling is done by comparing the migrated image (with some possible pre/post processings) with a second image obtained by remigrating the image (i.e., applying the normal operator on the image). Typically, this diagonal scaling is performed in some domains (physical, Fourier, curvelets, etc, see e.g. Rickett, 2003; Plessix and Mulder, 2004; Guitton, 2004; Symes, 2008; Herrmann et al., 2008).

In this paper, we use the third approach to estimate the inverse of the normal operator in curvelet domain by forming a quasi eigen-value decomposition of normal operator with curvelets as eigen-vectors. We show an example for application of our method on a portion of BP salt model dataset.

Theory

Ideally, the data used before migration, is primary only which is mathematically described as,

$$(1) \quad d = Km$$

in above equation, d is the data, K is the linearized Born scattering operator which is also called demigration operator and m is the reflectivity. Theoretically migration is the adjoint of scattering operator so when migration is applied to data,

$$(2) \quad m_{\text{mig}} = K^T d = K^T K m$$

The $K^T K$ is the normal operator which is also called Hessian operator in seismic imaging. In order to get m we need to invert this operator. In image-to-image based method, the migrated image once again remigrated which

means the demigration followed by migration is applied to it (i.e., $m_{\text{remig}} = K^T K m_{\text{mig}}$). Subsequently, using migrated and remigrated images an approximation for inverse of normal operator can be found. Mathematically, the estimation for the inverse normal operator can be written as,

$$m_{\text{mig}} = (K^T K m)^{-1} m_{\text{remig}} \quad (3)$$

$$= S^t W S m_{\text{remig}} \quad (4)$$

with m_{mig} the migrated image, m_{remig} the remigrated image (i.e., $m_{\text{remig}} = K^T K m_{\text{mig}}$), K the demigration operator and K^T the migration operator. The approximation consists of transforming (by S a linear transformation) the remigrated image, followed by a scaling with a positive diagonal matrix (W) an inverse transform it back to physical domain through the pseudo-inverse of S (denote by S^t). The performance of scaling methods depends on two components, namely:

- the choice of the appropriate domain for the scaling (i.e., the matrix S).
- the calculation of the filter coefficients, i.e., the diagonal of W , from the migrated image and remigrated image.

Rickett (2003), one of the pioneers of the scaling method first proposed by Claerbout and Nichols (1994), uses the identity basis ($S = \text{Id}$ with Id identity matrix) and calculated the filter coefficients by elementwise division of images. Aside from possible instability in this division, Rickett (2003) does not apply the appropriate preconditioning to the migration operator to be sure that operator is zero phase (see e.g. Herrmann et al., 2008; Symes, 2008). This may lead to inaccuracies in the region of the image where there are phase changes due to nature of the operator. Guitton (2004) improves this technique by applying scaling in a domain spanned by a filter bank. This approach allows him to treat dips locally and to impose smoothness amongst the filter coefficients.

However, he also does not correct for the order of the migration operator. Symes (2008) introduced a scaling approach during which the order of normal operator is corrected by filtering the image with a fractional inverse Laplacian, followed by the estimation of physical domain scaling using bicubic splines. He also imposes smoothness amongst the scaling coefficients. However, his approach is based on the assumption of the existence of well-defined dip in the migrated image since splines don't inherit any dip information in the approximation. In addition, the choice of spline for approximation of the normal operator is not mathematically justified.

Diagonal approximation of the normal operator

Theoretical implication: A 2D curvelet ϕ_μ is defined by its index $\mu = (j, k, \theta)$ with $j = 0, 1, 2, \dots$ the scale index,

$\theta = 0, 1, \dots, 2^{\lfloor j/2 \rfloor} - 1$ the orientation index ($\lfloor x \rfloor$ is the lower integer part of x), and the location index $k = (x, z)$. One of the important feature of curvelets is that the action of normal operator (i.e., $\psi = K^T K$) on a curvelet ϕ_μ is approximately mapped into the same curvelet within a scalar. Mathematically, we can derive following approximation,

$$(5) \quad \psi \phi_\mu \approx d_\mu \phi_\mu$$

with d_μ a positive scalar multiplier depend on the index $\mu \in M$, with M the index set, symbol \approx denote as "approximated by". In Herrmann et al. (2008), we theoretically and empirically showed this behavior by studying the behavior of curvelets at different scales, angles and location after applying the normal

operator. In addition, we proved a theorem which states that the above approximation (c.f., equation 5) becomes more accurate at finer scales (i.e., at higher spatial frequency).

Approximation formulation

Equation 5 suggests that curvelets are similar to eigenvectors of the normal operator. Therefore, we suggest a quasi-eigenvalue decomposition for the normal operator with curvelets as quasi-eigenvectors. This decomposition is similar to the Wavelet-Vaguellette Decomposition (WVD) proposed by (Donoho, 1995; Herrmann et al., 2008),

$$\psi_{\phi_\mu} \approx C^T D_\psi C_{\phi_\mu}, \quad (6)$$

where C and C^T are the curvelet transform and its adjoint (Candès et al., 2006), and D_ψ is a diagonal scaling matrix with elements of d_μ in Equation 5 with $\mu \in M$. Since curvelets are tight frames $C^T C = I$ and near unitary we can further assume that the similar approximation holds for inverse of normal operator with,

$$\psi_{\phi_\mu}^{-1} \approx C^T D_\psi^{-1} C_{\phi_\mu}, \quad (7)$$

As we mentioned, our method is based on the image-to-image fitting scheme. Comparing above equation with equation 3 results in $W = D_\psi^{-1}$, hence we have the following form,

$$m_{\text{mig}} \approx C^T W C m_{\text{remig}} \mapsto m_{\text{mig}} \approx C^T \text{diag}(v) w, \quad (8)$$

with $v = C m_{\text{mig}}$ and w representing the diagonal elements of W (i.e., $W = \text{diag}(w)$). The proposed method in equation 8 aims to find a curvelet-domain diagonal scaling vector (i.e., w in Equation 8) that approximates the action of the normal operator on the reference vector. Because the curvelet transform is redundant, the estimation of equation 8 corresponds to an underdetermined system of equations yielding non-unique solutions. To find a unique solution to this diagonal approximation problem we exploit additional properties of the operator we want to approximate. The symbols of the pseudo-differential operator, i.e., a space and spatial frequency dependent multipliers, are known to be smooth for smooth background velocity model (Stolk and De-Hoop, 2006; Herrmann et al., 2008; Stein, 1993), defining the Born-scattering operator and its adjoint. We use this property to formulate the diagonal estimation problem in terms of a nonlinear least squares problem yielding smoothness amongst neighboring curvelet coefficients.

$$\hat{z} = \arg \min_z J(z) = \frac{1}{2} \| m_{\text{mig}} - C^T \text{diag}(v) z \|_{l_2} + \frac{1}{2} k \| L z \|_{l_2}, \quad (9)$$

In above equation, $L = [D_x D_z D_\theta]$ is a sharpening operator, penalizing fluctuations amongst neighboring coefficients in z . The matrices $D_{x,z}$ contain the first-order differences at each scale in the x, z directions, and D_θ the first-order difference in the θ direction. These differences are scale-dependent because the spatial grid and angles of the curvelet partitioning of phase space both depend on scale. k is a smoothness control parameter.

The fit functional in Equation 9 is well-behaved and can be minimized by an efficient numerical optimization method. We chose to use Limited-memory BFGS (see e.g. Nocedal and Wright, 1999), knowing the gradient of minimization functional in equation 9 as follow,

$$\nabla_z J(z) = \text{diag}(v) C (C^T \text{diag}(v) z - m_{\text{mig}}) + 2k L^T L z \quad (10)$$

Examples

In order to investigate the effectiveness of our methodology, we perform a test on a subset of BP 2004 salt model dataset (Billette and Brandsberg-Dahl, 2004). To show improvement we focus on two different areas in the image to see how well our method performs.

Figure (1) zooms in the area left of the salt tooth,. Figures 1(a) and 1(b) shows the migrated and enhanced image around the potential reservoir zone located around (5000,30000)m, respectively. Figures 2(a) and

2(b) shows the migrated and enhanced image under the tooth shape salt flank. In both zones, we observe promising amplitude recovery results and significant amplitude boosts in the enhanced images. For this example, we used a two-way wave-equation reverse-time migration and modeling in time domain.

Conclusions

Compared to other approaches for migration amplitude recovery, some improvements in using the curvelet amplitude recovery method include the following,

- speeding up the calculation of the normal operator by diagonalizing it in curvelet domain.
- designing an efficient approximation that takes into account a laterally-variant velocity models and steep reflectors.
- replacing the ad hoc or trial-and-error estimation of migration amplitude with a method which has more theoretical and practical background.
- bringing the amplitude correction problem within the context of stable signal recovery.

Acknowledgements

Authors would like to thanks Chris Stolk at university of Amsterdam for providing us the Curvelet smoothing filter code. We also would like to thank Felix Herrmann at university of British Columbia for giving useful insight for completion of this work.

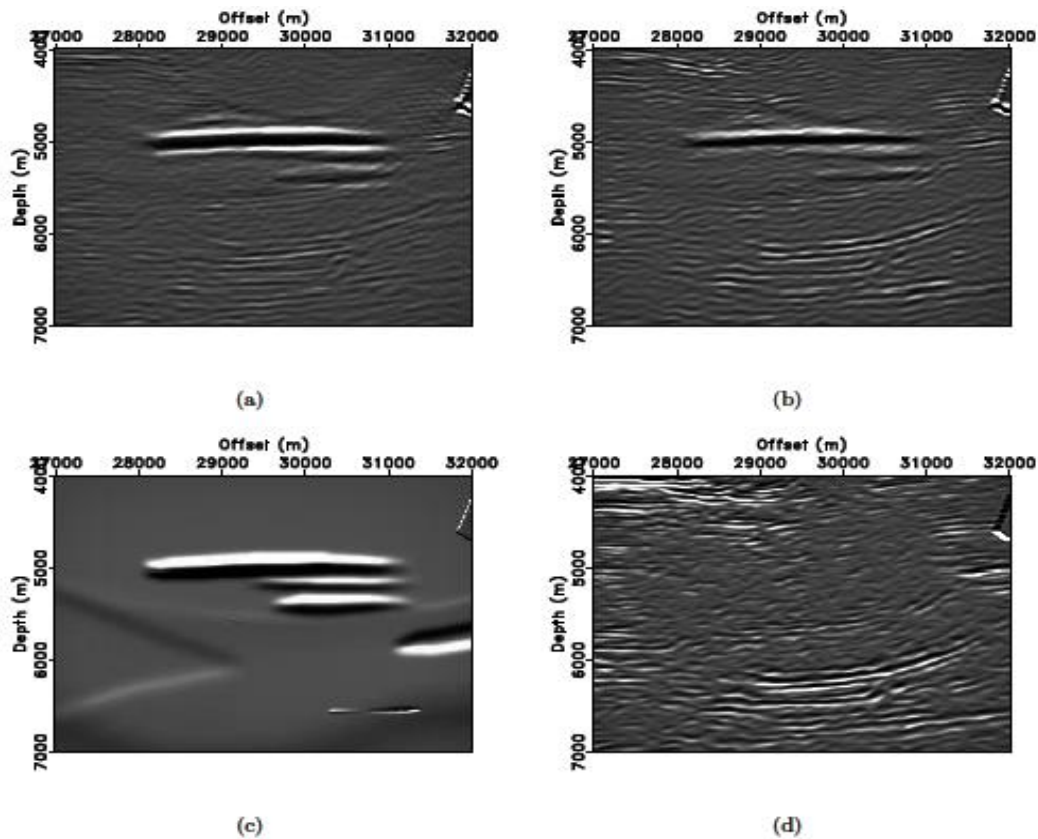


Figure 1: Comparison between the migrated and enhanced image in potential reservoir (a) migrated (b) enhanced, (c) Velocity differentiated along the vertical access, (d) Density differentiated along the vertical access.

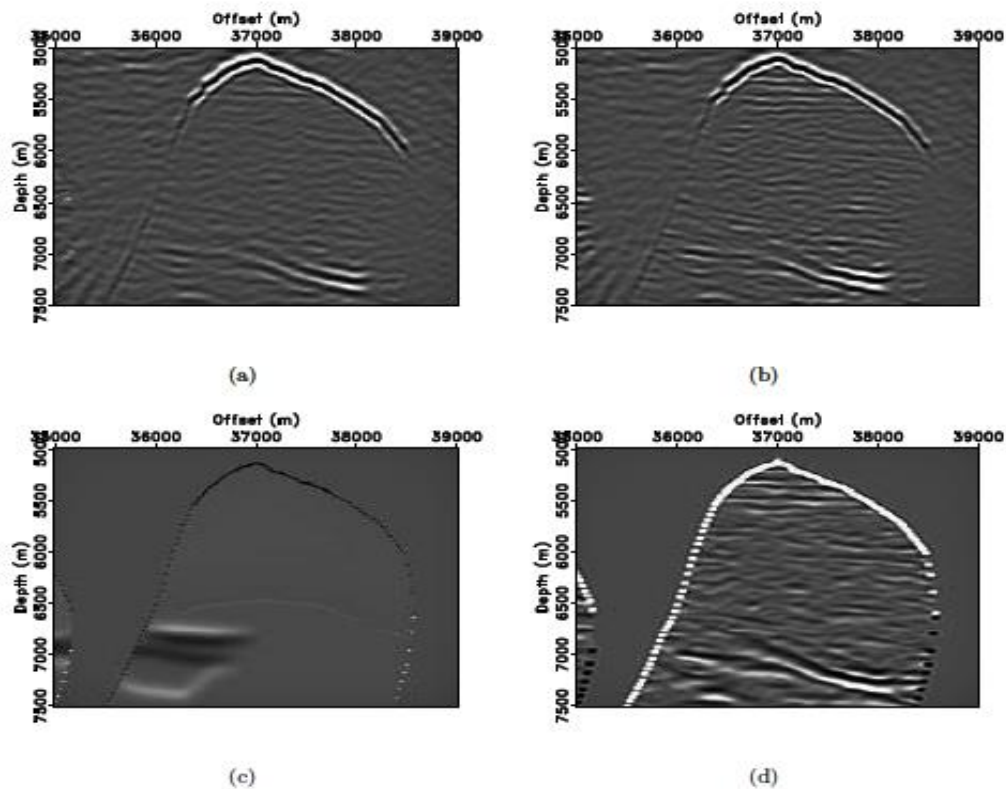


Figure 2: Comparison between the migrated and enhanced image under salt zone, (a) migrated (b) enhanced, (c) Velocity differentiated along the vertical access, (d) Density differentiated along the vertical access.

References

- Billette, F.J. and Brandsberg-Dahl, S., 2004, The 2004 BP velocity benchmark, 67th Annual Internat. Mtg., EAGE, Expanded Abstracts, B035, EAGE, Paris, France.
- Candès, E., L. Demanet, D. Donoho, and L. Ying, 2006, Fast discrete curvelet transforms: SIAM Multiscale Model. Simul., 5-3, 861–899.
- Chattopadhyay, S. and G. A. McMechan, 2008, Imaging conditions for prestack reverse-time migration: *Geophysics*, 73, S81–S89.
- Claerbout, J., 1985, *Earth soundings analysis, processing versus inversion*: Blackwell Scientific Publications.
- Claerbout, J. and D. Nichols, 1994, *Spectral preconditioning*: Technical Report 82, Stanford Exploration Project, Stanford University, Stanford, California, USA.
- Da Silva N., F.A., Costa, J.C. Schleicher, J., Novais A., 2011, 2.5D reverse-time migration: *Geophysics*, 76, 143–149.
- Gray, S., 1997, True amplitude seismic migration: A comparison of three approaches: *Geophysics*, 62, 929–936.
- Guitten, A., 2004, Amplitude and kinematic corrections of migrated images for nonunitary imaging operators: *Geophysics*, 69, 1017–1024.
- Herrmann, F., P. Moghaddam, and C. Stolk, 2008, Sparsity- and continuity-promoting seismic image recovery with curvelet frames: *Applied and Computational Harmonic Analysis* 24, 2, 150–173.
- J. C. Costa, F. A. Silva Neto, M. R. M. A. J. S. and A. Novais, 2009, Obliquity-correction imaging condition for reverse time migration: *Geophysics*, 74, S57–S66.
- Kuehl, H., and D. Sacchi, M, Wang, J, (2003) Least-squares wave-equation AVP imaging of 3D common azimuth data. SEG Technical Program Expanded Abstracts 2003: pp. 1039-1042

- Lu S., X. Li, A. Valenciano, N. Chemingui and C. Cheng, 2017, Broadband Least-Squares Wave-Equation Migration, SEG International Exposition and 87th Annual Meeting, Houston, Texas.
- Mulder, W. and R.-E. Plessix, 2004, A comparison between one-way and two-way wave equation migration: *Geophysics*, 69, 14911504.
- Nocedal, J. and W. Wright, 1999, *Numerical optimization*: Springer Verlag.
- Plessix, R. and W. Mulder, 2004, Frequency-domain finite-difference amplitude-preserving migration: *Geophysics. J. Int.*, 157, 975–987.
- Rickett, J., 2003, Illumination based normalization for wave-equation depth migration: *Geophysics*, 68, 208–221.
- Stein, E., 1993, *Harmonic analysis*: Vanderbilt University Press.
- Stolk, C. and M. De-Hoop, 2006, Seismic inverse scattering in the downward continuation approach: *Wave Motion*, 43, 579–598.
- Symes, W., S. C., B. Biondi, and G. F., 2004, Reverse time shot-geophone migration: The Rice Inversion Project, Department of Computational and Applied Mathematics, Rice University, Houston, Texas, USA.
- Symes, W. W., 2007, Reverse time migration with optimal check pointing: *Geophysics*, 72, SM213–SM221.
- Symes, 2008, Approximate linearized inversion by optimal scaling of prestack depth migration: *Geophysics*, 73, R23–R35.
- Trad D., 2017, Least squares Kirchhoff depth migration: important details, Geo-convention 2017, Calgary, Canada.
- Yang J., J. Huang, X. Wang, Z. Li, 2015, An amplitude-preserved adaptive focused beam seismic migration method, *Petroleum Science*, Volume 12, Issue 3, pp 417–427.